Journal of Energetic Materials
Publication details, including instructions for authors and subscription information:
http://www.informaworld.com/smpp/title~content=t713770432

Chemical characterization of plasma-treated propellant samples

P. Kaste[a]; A. Kinkennon[a]; R. Lieb[a]; A. Birk[a]; K. Del Guercio[a]; J. Newberry[a]; M. Schroeder[a]; R. Pesce-Rodriguez[a]
[a] U.S. Army Research Laboratory, Aberdeen, MD

To cite this Article Kaste, P. , Kinkennon, A. , Lieb, R. , Birk, A. , Guercio, K. Del , Newberry, J. , Schroeder, M. and Pesce-Rodriguez, R.(2001) 'Chemical characterization of plasma-treated propellant samples', Journal of Energetic Materials, 19: 2, 119 — 154
To link to this Article: DOI: 10.1080/07370650108216123
URL: http://dx.doi.org/10.1080/07370650108216123

CHEMICAL CHARACTERIZATION OF PLASMA-TREATED PROPELLANT SAMPLES

P. Kaste, A. Kinkennon, R. Lieb, A. Birk, M. Del Guercio,
J. Newberry, M. Schroeder, R. Pesce-Rodriguez
U.S. Army Research Laboratory, Aberdeen Proving Ground, MD 21005-5066

ABSTRACT

The morphological and chemical characterization of M30 propellant grains recovered after conventional or plasma ignition in interrupted closed bomb experiments has been performed. The capillary material used during plasma ignition was either polyethylene (PE) or polyethylene terephthalate (Mylar). Propellants were extinguished at pressures between 35 and 100 MPa. The samples are of interest due to previous reports of apparent burning rate augmentation with plasma ignition of M30, compared to conventional ignition, in non-interrupted closed bomb experiments [1]. Birk [2] has reported that burning rate augmentation appears to occur during the plasma event, but there was no evidence for post-plasma augmentation. Birk has also analyzed vivacity curves from plasma-ignited M30 and the data indicated that the grains appear to burn regressively, suggesting an increase in surface area was generated

Journal of Energetic Materials Vol. 19, 119-154 (2001)
Published in 2001 by Dowden, Brodman & Devine, Inc.

beyond that expected from normal grain burning [2]. In the current work, differences between extinguished grains from conventional and plasma ignition were primarily physical or morphological in nature. For the extinguished grains from PE plasma ignition there appeared to be a stripping of NQ crystals in the perforations. Along the outer surfaces of the grain ignited with plasma, hot embedded particles and increased surface area were observed, and the melt layer was immeasurably thin. Although extensive chemical characterization has been performed, there appears to be very little chemical difference between the burned surfaces of the plasma and conventionally ignited samples. The SEM analysis of the perforations showed that NQ depletion in the perforations was most evident at the lowest blowout pressure used (35 MPa) and seemed to diminish at higher pressure, apparently becoming obscured by "normal" burning processes. Thus, it appears that plasma-propellant interactions and associated effects occur only very early during ignition. This is consistent with the fact that few differences in the chemical composition are observed for plasma and conventionally ignited samples. A depletion of NQ in the perforations may contribute to a true burning rate augmentation through chemical reactions. However, a true chemical burning rate augmentation as the only mechanism for the M30 non-interrupted behavior would not be consistent with regressive burning.

INTRODUCTION

The interaction of plasmas with solid propellants is being investigated using an interrupted closed chamber capable of either plasma or conventional black powder ignition. The ultimate goal is to understand plasma-propellant interactions so that plasma ignition may be used for improved gun systems. Low-density plasmas offer the potential for enhanced gun performance through short ignition delays, efficient ignition of high energy density charges, and the ability to tailor the mass generation rate of solid gun propellants so that the temperature sensitivity in gun systems is minimized. Replacing conventional igniters could also improve vulnerability properties. In previous, non-interrupted, closed bomb analyses, the effect of plasma ignition on propellant burning rate was investigated, and it was reported [1] that for M30, a 33% increase in burning rate over the range of 100-220 MPa occurred with plasma ignition, relative to conventional ignition with polyethylene capillaries. Apparent burning rate augmentation is also observed with Mylar capillaries, but to a lesser extent. The plasma augmentation of JA2 burning rate was insignificant. Researchers in the international community have also reported augmentation of the burning rate with nitramine-based composite propellants [3]. In the initial, non-interrupted burn studies with M30, the plasma was generated by ablating a polyethylene (PE) capillary [1].

In this work, interrupted burn experiments with conventional or plasma ignition have been performed for the dual purpose of: a) determining whether the increase in burning rate for M30 was intrinsic to the propellant or the result of an increase in surface area due

to, for example, fracture [4] or porous burning; and b) characterizing extinguished grains to understand the ignition and combustion chemistry that occurs with the two igniters. The approach was to repeat key experiments from Del Guercio [1] with M30 and JA2 propellant but interrupt the burning at 35, 75, and 100 MPa and collect the extinguished propellant for physical examination and chemical analysis. The interrupted closed bomb experiment offers a means of studying basic plasma-propellant interactions under well-defined conditions of plasma energy and power input, pressure profile, and proximity of the grains to the plasma. Since the blowout pressure can be varied, the grains can be studied after ignition when plasma-propellant interactions would be dominant, or at higher blowout pressures when the propellant burning would be dominant. Morphological and chemical characterization of residual propellant from both plasma and conventionally ignited samples has provided a method for studying differences in plasma and conventional closed bomb ignition.

EXPERIMENTAL

1. Closed Bomb Firings. Propellant samples for closed bomb analysis consisted of seven-perforated grains of M30 or JA2 with a diameter, length, and perforation diameter of nominally 0.75, 1.5, and 0.07 cm, respectively. Closed bomb analyses of M30 and JA2 were performed in a 3.81-cm inner diameter (ID) closed bomb with a volume of 129 cm^3. For all firings, a typical propellant charge weighed 32 gm. For extinguished propellant measurements, the addition of the interface of the bomb to the evacuation chamber yielded a total closed bomb area of 150 cm^3 (Figure 1). The expansion chamber consists of a 240-liter tank with a 2.5-cm-diameter blowout area interfaced to the closed bomb. Rapid extinguishment of the propellants occurred due to the sudden expansion into the evacuated tank. Soft capture of the propellant was achieved with a lining of thermally resistant polyurethane foam. In the case of plasma ignition, a perforated straw with 24 holes was used to facilitate uniform distribution of the plasma around the propellant (Figure 2). In the conventional mode, an electric match was used to ignite 0.6 gm of black powder confined in a plastic straw with the propellant distributed in two tiers concentrically positioned around the straw (Figure 3). The plasma was generated by an electrical pulse to a nickel fuse wire, which was rapidly vaporized. This resulted in ionization of the capillary liner (PE or Mylar), and a high current discharge was sustained. The time interval for injection was between 0.9 and 1.2 ms. The electrical pulse was generated with a 400-kJ capacitor-based pulse-forming network, with a charging voltage of 4 kV and an output energy of up to 29.3 kJ. The chamber was equipped with one or two 607-C4 Kistler pressure transducers.

2. High-Pressure Liquid Chromatography (HPLC)-UV Analysis. HPLC was used to quantify the components, except for nitrocellulose(NC), of virgin and extinguished grains of JA2 and M30. For JA2 propellant, levels of the plasticizers (nitroglycerine (NG) and diethylene glycol dinitrate (DEGDN)) and its stabilizer, Akardite II, were determined. For M30, NG and the crystalline oxidizer nitroguanidine (NQ) were determined. Propellant grains were microtomed into 40 μm thick cross-section samples, extracted twice for at least 2 hrs with 2-3 ml of 80:20 acetonitrile (CH_3CN): water (H_2O). Extractions were prepared in triplicate. An additional extraction was performed overnight and the solid residue was rinsed with a fourth aliquot. The total dilution volume was 10 ml. Samples were filtered through 0.45-μm filters. Virgin samples of JA2 and M30 were used to prepare the calibration curves and were prepared in duplicate. The chromatographic parameters are listed in Table 1. M30 samples were run with a detector monitoring both 260 nm for the NQ analysis and 210 mg for the NQ analysis. NQ elutes with the extraction solvent, but at 260 nm, only NQ was detected, which improved the error in the analysis.

Table 1. Chromatographic Parameters for JA2 and M30 Component Analysis

Chromatograph	Isco Model 2350 Pump
Stationary Phase	Alltech C18 Econosphere 5u Cartridge
Mobile Phase	$CH_3CN:H_2O$, 60:40
Flow	Rate 0.5 ml/min
Injection	10-ul Fixed-Loop Injector
Detector	Spectra Physics FOCUS @ 210 nm; 260 nm for NQ
Data Collection	ThermoSeparation Products PC1000 Software

3. Liquid Chromatography-Mass Spectroscopy (LC-MS). LC-MS was used to investigate decomposition of the components of JA2 and M30. A Hewlett-Packard 1090 liquid chromatograph was used with a 59980B LC-MS interface and 5989B mass spectrometer. Outer shavings of the propellant grains were extracted overnight. Extraction solvents were ether (for JA2) and 2:1 methanol:water (for M30). Both solvent systems were chosen to exclude NC in the extract. The ether was evaporated, and the JA2 extracts were re-dissolved in 2:1 methanol:water. Samples were passed through cellulose filters (0.2 μm) prior to injection of 25 uL aliquots. A C18 microbore column (100 x 2.1 mm; 5 μm bead size) was used in the separation. The elution solvent was 50:50 MeOH:water at 0.3 ml/min. The mass spectrometer was run in the electronic ionization mode and ions between 34 and 200 m/z ratio were monitored.

4. Scanning Electron Microscopy (SEM). Micrographs of virgin and extinguished grains were examined to establish any morphological differences between grains ignited by conventional or plasma sources. The grains were cold-fractured along the longitudinal grain axis to expose the burned surfaces of the perforations, a cross-section of the burning surfaces, and the unburned propellant below this surface.

The lateral exterior burn surfaces were also examined. The prepared specimens were sputter coated with gold-palladium for 20 to 30 sec at 30 mA. An International Scientific Instruments SEM, model ISI-SS-40, was used with a 10keV electron beam. The images were captured on Polaroid sheet film.

5. FTIR Analysis. Micro-reflectance FTIR was used to obtain spectra of the propellant surface (i.e., about top 10 μm) with no modification of the sample. FTIR analyses were performed using a Mattson Polaris spectrometer operating at a resolution of 4 cm^{-1}. The reflectance spectra were obtained using a Spectra-Tech (Shelton, CT) microreflectance attachment with 32X IR objective and signal averaging 200 scans. Aluminum foil was used to collect the background spectra. Data were reduced with FIRST (Mattson) software; the Kramers-Kronig transformation algorithm was performed on the transmittance spectrum to obtain spectra in absorbance units. Samples for micro-reflectance must be flat, since curvature may distort the focus. Typically, JA2 samples were cut with a razor; M30 samples were prepared by microtoming.

6. X-Ray Fluorescence (XRF) Spectroscopy. XRF spectroscopy was performed on the extinguished grains in order to identify metals present in the plasma that may be incident on the propellant samples. Before obtaining XRF spectra, the propellant grains were cooled to dry ice temperature and split with a knife blade. The knife blade was laid vertically against the propellant grain, struck with a hammer, and a clean split was obtained. The split samples were coated with carbon using a carbon-coating instrument (SPI Supplies Inc, West Chester, PA). The propellant-to-carbon fiber distance was greater than 3.5 cm, and a low voltage was used to minimize exposure

of the sample to heat. Spectra were obtained using a Kevex model 3600-0374 XRF detector interfaced to a Kevex Delta Class Analyzer with Kevex Quantex software, version V. The XRF was interfaced to a JEOL 820 scanning electron microscope (SEM).

RESULTS

1. Closed Bomb Firings. Initial, non-interrupted experiments in which the propellant was completely burned showed that the apparent plasma burning rate augmentation of M30 was greater for the PE capillary compared to the Mylar capillary (Figure 4).

The power curve was considered when evaluating each trial with plasma ignition. For burning rate determination, comparable energies and rise times were desired. Figure 5 shows two plots for which the initial rise is similar, but the area under the curves is much different, yielding input energies of about 18 kJ for the M30 samples and 29 kJ for the JA2 samples. The initial rise is comparable for all samples, so that the strain rates applied to the propellants would be expected to be comparable. Excessive strain rates that might cause fracture as an artifact were thereby avoided.

The P-t curves for the M30 and JA2 samples ignited by plasma are shown in Figure 6, for blowout pressures of nominally 35 and 100 MPa. P-t curves for conventionally ignited M30 are also shown, and are evident from the longer time-to-burst of about 10 ms at 60 MPa. Also apparent is the uniform curvature due to the regular mass generation of the conventionally ignited propellant. In contrast, propellants ignited by plasma show a sharp increase in pressure within the first 1-2 milliseconds due to the sudden plasma impulse, followed by a more

typical pressure increase when normal propellant burning takes over. In the case of JA2, early experiments with the PE capillaries were used for plasma generation, and curves with overlying traces for the initial pressure rise were obtained. However, because none of the many firings with PE yielded overlapping curves for M30, Mylar capillaries were used for the M30 series.

Originally, it was hoped that a propellant burning rate could be computed using BRLCB [5] for each closed bomb trial using the P-t curves and the changes in the dimensions of grains [6]. However, the fact that the P-t curves of the plasma-ignited grains showed an initial rapid pressurization made the analysis more complicated. Therefore, for a given propellant, two firings were selected that had similar plasma power conditions and pressure-time histories, but were extinguished at two different pressures. (See Figure 6, ETC curves for M30 or JA2.) The recovered grains from both firings were measured to determine the extent of regression between the two blowout pressures. The regression between the two blowout pressures was also calculated assuming conventional burn rate parameters. Comparison of the calculated and measured regression distances gave an indication of the extent of the intrinsic post-plasma burning rate augmentation. Typically, during the plasma pulse the pressure would rise to about 30 MPa for PE capillaries and about 20 MPa for Mylar capillaries. It is noted that pressures comparable to the 20-30 MPa initial pressure spikes were generated in analogous closed bomb trials in which no propellant was used, showing that the pressure increases are due to generation of the plasma [7].

For both M30 and JA2, no was evidence was found of burning rate augmentation after the plasma event (i.e. the measured grain

regression was consistent with that calculated using conventional burn rate parameters for these propellants). Thus, it appears that the post-plasma burn rates are not intrinsic. For both M30 and JA2, grain regression at 35 MPa was consistently greater than predicted based on conventional burning rates, which is evidence that there is burning rate augmentation (40-120%) during the plasma event. Details of this analysis are provided in [2].

Burning occurred to a greater extent in the samples ignited with black powder than with the plasma due to the fact that, with plasma-ignited samples, a significant fraction of the total pressure was due to plasma injection, rather than propellant burning. This initial plasma pressurization occured rapidly, leaving a shorter effective time for propellant burning to occur (about 4-6 msec at 60 MPa), compared to conventional ignition (about 11 msec at 60 MPa; see Figure 6). This occurred whether Mylar or PE capillaries were used in the plasma ignition. For M30 grains recovered at nominally 35 and 60 MPa, the grain regression measured for plasma ignited samples (Mylar capillaries) was 0.23 and 0.33 mm respectively, while for conventionally ignited samples, the regression measured for the same blowout pressures was 0.37 and 0.62 mm respectively.

2. **HPLC.** Virgin and extinguished samples of JA2 and M30 from conventional and plasma (PE-based capillary) ignition were analyzed by HPLC. The components of JA2 (the plasticizers, NG and DEGDN, and stabilizer, Akardite II) and M30 components (NG and crystalline NQ) were analyzed. No decomposition products were detected from either virgin or extinguished grains. Moreover, no significant difference in the plasticizer (NG, DEGDN) levels of virgin for extinguished JA2 propellant (either from conventional or plasma ignition) was

observed. Nor does M30 show any difference between the virgin and extinguished grains.

3. LC-MS. The extinguished samples of JA2 and M30 at various blowout pressures were analyzed; virgin samples were included as references. Only the outer surfaces of the grains were sampled in order to obtain the greatest possible concentration of any decomposition products present. The LC-MS chromatograms obtained for virgin and conventionally ignited JA2 were indistinguishable. For the plasma-ignited sample, an early eluting peak (less than 1 min) is observed with the plasma sample. Although the peak overlaps a methanol impurity peak (determined from a separate analysis of methanol; not shown), the peak is too large to be due to this component alone. Major peaks in the mass spectrum of this unknown were 63, 77, 120, and 148 m/z. It is noted that the nitrate esters (e.g., DEGDN and NG) typically yield a 46-m/z fragment, presumably due to ONO, and this fragment was not detected in the unknown. Thus, if it is a decomposition product of the NG or DEGDN, it would apparently be totally denitrated. The chromatograms of the M30 components were also virtually identical, and no decomposition product was detected.

4. Scanning Electron Microscopy. Extinguished surfaces have been studied previously [8], and it has been noted that many combustion features are preserved on surfaces that undergo a rapid pressure reduction. The flame is rapidly blown away from the surface, which quickly solidifies, leaving most of the burning surface features intact. SEM micrographs from this study revealed several interesting features. The exterior lateral surfaces of many of the extinguished grains from both the plasma and conventional ignition sources

appeared very similar except for one feature. In plasma ignition, the grains showed evidence of burning caused by hot particles being sprayed onto the grain surface, as shown in Figure 7, 90X. Also, several grains showed very irregular, nonprogrammed burning (Figure 7, 5X). These phenomena would increase the surface area, and would give the appearance of a higher burning rate during the early stages of the propellant combustion. However, since the augmentation is caused by increased surface area, the apparent burning rate will be lowered in later stages of burning, as the resulting surface area is reduced due to the intersection (burn through and crossing) of burning surfaces.

Another interesting feature was noted on the burning surfaces within the perforations. Most burning surfaces of extinguished propellant appeared as shown in Figure 8, which depicts a conventionally ignited grain. Note that the surface is smooth, indicating melting. However, in Figure 8 there seemed to be no indication of melting with plasma ignition. Moreover, there appeared to be a series of grooves that conformed to the size of NQ particles (about 5 μm in diameter, 50-200 μm long). Stereoscopic pictures confirmed the presence of grooves. This suggests a different process for the plasma-ignited samples that caused the NQ crystals to vacate the matrix. It is noted that were much less prominent at higher pressure (100 MPa, not shown) and the surface appeared more like the conventional. This is consistent with the burning mechanisms returning to similar processes at higher pressures.

One other observation on the morphology of the M30 propellant is worth noting. While most propellants have measurable melt layers that range from 2 to 30 μm in thickness, the melt layer was too thin

to be measured. The evidence for a melt layer is shown in Figure 8 for the conventional sample, as noted above. However, the propellant went from the outer melted surface to an unburned structure regardless of the ignition source, without any measurable transition depth.

5. FTIR Analysis. Microreflectance FTIR analysis of propellant grains was performed to determine differences in chemistry with plasma vs. conventional ignition. The lateral, external surfaces of JA2 grains ignited with plasma or black powder showed evidence of aldehyde formation (appearance of a carbonyl band at 1735 cm^{-1}) due to denitration of the nitrate esters (Figure 9). The carbonyl formation was detected at the higher blowout pressures but was not apparent at 35 MPa (Figure 9). Thus, denitration appears to be related to extent of burning, not to the type of ignition.

Since, for M30, NQ depletion in the perforations was observed in the SEM analysis, the microreflectance spectra of both the perforated regions and lateral surfaces of the extinguished M30 grains were obtained. The results for the lateral surfaces are shown in Figure 10a. The NQ diminished with increasing pressure in both conventional and plasma-ignited samples. Conventionally ignited samples at 75 MPa burned (i.e., regressed) the most, and for these samples NQ at the surface is virtually eliminated. Thus, the depletion of NQ at the surface at pressures up to 100 MPa appears to be related to extent of regression, rather than to the ignition method. This trend was the same whether the plasma ignition was initiated with a PE or Mylar capillary.

The microreflectance spectra of the M30 perforated regions were also obtained. Figure 10b shows the results for PE capillary plasma ignition, which are similar to those for the lateral surfaces (i.e. greater NQ reduction occurs at higher pressure). This trend was the same whether plasma or conventional ignition was used.

This is seemingly in contrast to the SEM results (previous section), which showed that, particularly at 35 MPa, NQ particles appeared to be stripped from the perforations. The SEM and FTIR results can be resolved by the fact that the NQ crystals are locally concentrated and aligned along the direction of extrusion near the surface of the perforations. Previous SEM results [9] have shown that bundles of NQ crystals align along the perforation axis, thinly coated in binder, with each crystal being approximately 5 μm in diameter. Thus, it is very feasible that after the outer NQ crystals are removed, the new surface generated is equally rich in NQ crystals. At low pressure blowout (35 MPa), regression due to normal burning has apparently not removed the crystales. The micro-reflectance spectra are proportional to the concentration of NQ crystals in about the top 10 μm of the surface. Thus, the FTIR spectra are comparable for virgin and plasma-treated samples, whereas the SEM, with topological capability, detects the NQ crystal loss [9]. It is also noted that surface alignment of the NQ crystals does not occur to the same extent along the outer, lateral surfaces, so that such NQ stripping is specific to the perforated regions.

M30 samples that were ignited with plasmas using Mylar capillaries were also examined. Unlike the plasma-ignited samples for which polyethylene capillaries were used, Mylar capillaries resulted in less deposition of residue on the surface of the grains,

making microreflectance analysis through the residue possible. The results differed from those obtained with PE capillaries in that a carbonyl band was apparent when the Mylar capillary was used, suggesting denitration of the nitrate esters to the aldehyde. Unlike the case of JA2, however the carbonyl band in M30 did not appear in any of the conventionally ignited samples examined (Figure 11). The band was found (and was most intense) in all the spectra from samples extinguished at 35 MPa, and in some of the samples up to 80 MPa; it was not found at the highest pressure used, 100 MPa. This may suggest a different mechanism for M30 vs. JA2. With JA2, the normal burning process appears to augment aldehyde formation, but with M30 ignited with using Mylar capillaries, the aldehyde appears to be formed early and is diminished by the normal burning process.

The other feature that can be observed in Figures 11 is that the spectra of the extinguished samples show distortions in the baselines near 1815 cm^{-1}, due to the fact that the spectra were sampled through a carbonaceous residue. Thus the residue is not totally specular, which is the ideal situation for applying the Kramers-Kronig (KK) [10] transformation to obtain the absorbance spectrum.

6. XRF Spectroscopy. XRF was used to detect metals from the closed bomb hardware which may impinge on the sample. The XRF results for the outer, lateral surfaces and for the perforated surfaces of the extinguished grains were examined. Iron from the closed bomb hardware was found on the outer surfaces for both plasma (PE capillary) and conventionally ignited samples. The results for M30 are shown in Figure 11, inserts. In addition, Cu from caps on the electrodes was deposited on the plasma-ignited samples. The results for the perforated regions were quite different for conventional vs.

plasma ignition (Figure 12, b and c). As had been observed on the outer surface, the plasma-ignited sample shows the presence of Fe and Cu inside the perforations. However, although Fe was found on the outer surface of the conventionally ignited sample (Figure 12, insert), it is not observed inside the perforations. The spectrum of a virgin grain shows no significant Cu or Fe present (Figure 12a).

The presence of metals inside the perforations in the case of plasma ignition, while none is found with black powder ignition, may suggest a greater force penetrates inside the perforations during plasma ignition. This is consistent with SEM results that show that NQ in M30 is stripped by plasma ignition, and not by conventional ignition.

CONCLUSIONS

In order to better understand the basic mechanisms of plasma-propellant interactions, the morphological and chemical characterization of extinguished M30 propellants from conventional and plasma (PE and Mylar) ignition has been performed. The ultimate goal of this work is to develop design rules for plasma ignition of propellants so that increased performance and reduced vulnerability may be realized. Although few differences between conventional and plasma ignition were detected in the chemical analyses, important physical and morphological differences were observed. An initial rapid pressure increase was evident in the P-t traces for plasma ignition, resulting in the blowout pressure being achieved more quickly, so that there was less time for the propellants to burn. Thus, extinguished grains from conventionally ignited samples regressed to a greater extent than those ignited with plasma.

Moreover, the initial pressure rise might have resulted in a shock formation in the closed bomb. A similar system in which the plasma was generated with an ablating capillary has been modeled for open expansion into air [11]. The model revealed an underexpanded jet, with a precursor shock, a barrel shock that reflects at a triple-point and a Mach disk. Although differences exist between the open-air and closed bomb systems, including boundary and electrical characteristics, it seems reasonable that some sort of shock or force occurs that modifies the solid propellant, and is greater for plasma than for black powder ignition. Dynamic compressive mechanical properties testing [12,13] has shown that M30 is more brittle than JA2. Thus, it has been proposed [14] that the apparent burning rate augmentation of M30 was due to grain fracture. Nonetheless, no widespread fracturing were observed. This is important in that propellant fracture has severe adverse implications for gun systems.

Several other observations related to the propellant surface are consistent with an increased interaction of the plasma with the propellant, compared to black powder:

a) NQ crystals appear to be stripped from the perforation axes in plasma-ignited M30 propellants. The normal melt layer observed for conventionally ignited samples is not observed with plasma ignition.

b) Metals from the closed bomb hardware are apparent in the perforations of the plasma-ignited samples (PE), but are not found in the conventionally ignited samples.

c) Irregular burning is found on the lateral surfaces of some plasma-ignited M30 propellant grains, possibly due to ablation.

Although extensive chemical characterization has been performed,

including P-GC-MS, LC-UV, LC-MS, and FTIR analyses, there appear to be very few chemical differences between the burned surfaces of the plasma and conventionally ignited samples. Efforts to isolate products promptly after sampling were undertaken to improve the sensitivity of the analyses; nonetheless, few specific differences between conventional and plasma ignition were identified.

In fact, it may be that any differences in chemical interactions that occur initially with plasma and conventional ignition are obscured by later burning processes, so that there are few decomposition products remaining on the extinguished propellant surfaces. This is supported by the SEM analysis, which show that NQ depletion in the perforations was most evident at the lowest blowout pressure used (35 MPa) and seemed to diminish at higher pressure, apparently becoming obscured by "normal" burning processes. Thus, plasma-propellant interactions, and associated effects, may occur only very early during ignition. This is consistent with the results reported by Birk [2] that the increase in burning rate due to the plasma occurs during, not after, the plasma event. It is also consistent with a greater force (evidenced by the initial high slope of the P-t curve) or possible shock (analogous to the open air plasma formation) occurring early in the plasma process).

Birk has also analyzed the vivacity curves from the closed bomb trials of the samples studied in this work. Vivacity curves [15] that slope upward with increasing pressure indicate progressive burning, as would be expected from 7-perforated grains. Downward-sloping curves indicate regressive burning, which if observed for 7-perforated grains implies an increase in surface due to some mechanism other than normal grain burning. Birk has found that JA2

grains appear to burn progressively, while M30 appears to burn regressively. An increase in surface is consistent with regressive burning.

The source of the increased surface area is being investigated. Kooker [14] has performed simulations showing that the shape and magnitude of the burning rate curves deduced from ETC closed-chamber experiments were reproduced with a modest amount of grain fracture. It is feasible that an increase in surface area by means other than grain fracture (e.g., surface ablation, embedded particles, microcracks etc.) could yield similar results. For example, the SEM photographs shown in Figure 7 reveal surface area generation not typical of normal burning of perforated grains. Whether the phenomena observed in the SEM photographs could still generate sufficient surface area to account for the burning rate augmentation is under investigation. A depletion of NQ in the perforations will also be investigated as a means of contributing to a true burning rate augmentation through chemical reactions. However, a true chemical burning rate augmentation as the only mechanism for the M30 non-interrupted behavior (Figure 4) would not be consistent with regressive burning.

The plasma dependence on capillary composition is also being further investigated through experiments (7) and modeling (16). The peak pressure measured in empty chamber trials, given comparable plasma energy, is less for Mylar [4] than for PE capillaries. The physical phenomena that might account for this observation are complex. Compared to PE, Mylar produces a more dense plasma, but with lower exit velocity. The calculated temperatures of the effluent for Mylar and PE are also comparable (16). Thus, in spite of their different elemental composition, the gas dynamics for PE and

Mylar capillary plasmas may be similar. A more detailed analysis is planned.

The capillary residue is clearly different for the two materials. Mylar generates significantly less residue, presumably because Mylar contains oxygen, which assists in the conversion of carbon and hydrogen to permanent gases. Hot particles formed during the generation of the residue may contribute to a true burning rate augmentation, which occurs during the plasma event by processes that could include an increase in surface area due to embedded or erosive particles, increased heat conduction, or other mechanisms.

SUMMARY

In extinguished closed bomb analyses, burning rate augmentation of solid propellants with plasma ignition was found to occur during, but not after, the plasma event. An initial rapid pressure rise, detection of metals in the perforations, stripping of NQ from M30 propellants, irregular surface burning (possibly due to ablation), and hot embedded particles have been observed with plasma, but not with conventional ignition, suggesting a more forceful process for plasma ignition. Nonetheless, no evidence of fracture or microcracks were observed in grains extinguished after plasma ignition. Moreover, chemical analyses of extinguished grains have not revealed any identifiable differences between plasma and conventional ignition, very possibly because any early chemical interactions are obscured by normal burning processes occurring later. Experimental and modeling efforts are in progress to understand the phenomena responsible for burning rate augmentation during the plasma event, and the apparent burning rate augmentation observed in non-

interrupted closed bomb experiments. Candidate mechanisms include, but are not limited to, surface area generation (e.g., embedded particles or non-programmed burning, both observed in the SEM), heat conduction by hot particles, heat generation by choked shock waves, and ablation by shock waves.

ACKNOWLEDGMENTS

Dr. D. Kooker (ARL, APG, MD) spent much time in helpful discussions and his technical insights are very much appreciated. Dr. Michael McQuaid (ARL, APG, MD) is thanked for his consultations in the area of capillary physics. Dr. Michael Nusca (ARL, APG, MD) is thanked for his discussions regarding plasma flow and shock formation.

REFERENCES

1. Del Guercio, M. "Propellant Burn Rate Modification by Plasma Injection." 34th JANNAF Combustion Subcommitte Meeting, Vol. 1, pp. 35-42, West Palm Beach, FL October 1997.

2. Birk, A., M. Del Guercio, A. Kinkennon, D. E. Kooker, and P. J. Kaste. "ETC Closed-Chamber Interrupted-Burning Tests with JA2 and M30 Solid Propellants." 36th JANNAF Combustion Meeting, NASA Kennedy Space Center, FL, 18-22 October 1999.

3. Woodley, C. R., and S. Fuller. "Apparent Enhanced Burn Rates of Solid Propellants Due to Plasmas." 16th International Symposium on Ballistics, pp. 153-162, San Francisco, CA, 23-28 September 1996.

4. D. E. Kooker. "Burning Rate Deduced form ETC Closed-Chamber

Experiments: Implications for Temperature Sensitivity of Gun Systems." 35th JANNAF Combustion Subcommittee Meeting, CPIA Publication 680, Vol. II, pp. 201 - 217, December 1998.

5. Oberle, W., and D. Kooker. "BRLCB: A Closed-Chamber Data Analysis Program." ARL-TR-36, U.S. Army Research Laboratory, Aberdeen Proving Ground, MD, January 1993.

6. Kaste, P. J., A. E. Kinkennon, R. A. Rodriguez, M. Del Guercio, D. Devynck, A. Birk, S. L. Howard, and M. A. Schroeder. "Chemical Analysis of Extinguished Solid Propellants from an Interrupted Closed Bomb with Plasma Igniter." 35th JANNAF Combustion Meeting, Tucson, AZ, 7-11 December 1998.

7. Del Guercio, M. "Electrothermal-Chemical Closed Chamber Characterization of Plasma Capillaries." 36th JANNAF Combustion Meeting, NASA Kennedy Space Center, FL, 18-22 October 1999.

8. Lieb, R., and C. Gillich. "Morphology of Extinguished Monolithic JA2 Grains Fired in a 30-mm Solid Propellant Electrothermal-Chemical (SPETC) Gun." ARL-TR-606, U.S. Army Research Laboratory, Aberdeen Proving Ground, MD, November 1994.

9. Lieb, R., P. Kaste, A. Birk, A. Kinkennon, R. Pesce-Rodriguez, M. Schroeder and M. Del Guercio. "Analysis of Burning Rate Phenomena and Extinguished Solid Propellants from an Interrupted Closed Bomb" 18th International Ballistic Symposium, San Antonio, TX, 16-19 November 1999, in press.

10. Lieb, R., "Nitroguanidine Morphology in Extruded Gun

Propellant," Technical Report BRL-TR-2812, US Army Ballistic Research Laboratory, APG, MD, June 1987.

11. Robinson, T. S. Proc. Physics Soc. London Ser. B., 65, 910, 1952.

12. Nusca, M. J., and M. J. McQuaid. "Modeling the Open-Air Plasma Jet from an ETC Igniter Using a Multi-Species Reacting Flow CFD Code." Proceedings of the 35th JANNAF Combustion Subcommittee Mtg, October 1999.

13. Gazonas, G. A. "The Mechanical Response of M30, XM39 and JA2 Propellants at Strain Rates from 10^{-2} to 250 Sec-1." BRL-TR-3181, U.S. Army Ballistic Research Laboratory, Aberdeen Proving Ground, MD, January 1991.

14. Lieb, R. J., and M. G. Leadore. "Mechanical Failure Parameters in Gun Propellants." Technical Report, BRL-TR-3296, U.S. Army Ballistic Research Laboratory, Aberdeen Proving Ground, MD, November 1991.

15. Klingaman, K.W., and J.K. Domen. "The Role of Vivacity in Closed Vessel Analysis." JANNAF Propellant Development and Characterization Subcommittee Meeting, Patrick AFB, FL, April 1994.

16. Kooker, D. E. "Burning Rate Deduced From ETC Closed-Chamber Experiments: Implications for Temperature Sensitivity of Gun Systems." *35th JANNAF Combustion Subcommittee Meeting*, Tucson, AZ, December 1998.

17. McQuaid, M. A., "Characterization of the Discharge from an Ablating Capillary Arc Ignition System Equipped with a Poly(Ethylene Terephthalate) Liner)." ARL Report, in press.

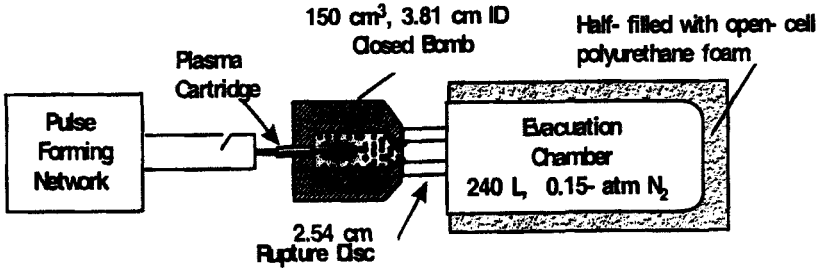

FIGURE 1.

Apparatus for Extinguished Closed Bomb Experiments with Propellant Soft-Capture.

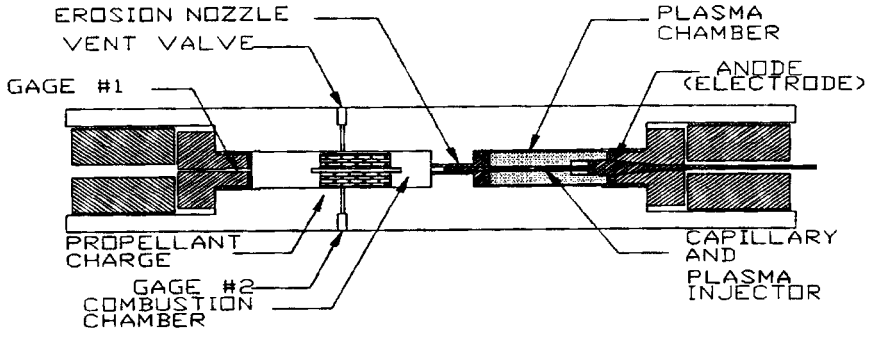

FIGURE 2. Schematic of the Plasma Igniter.

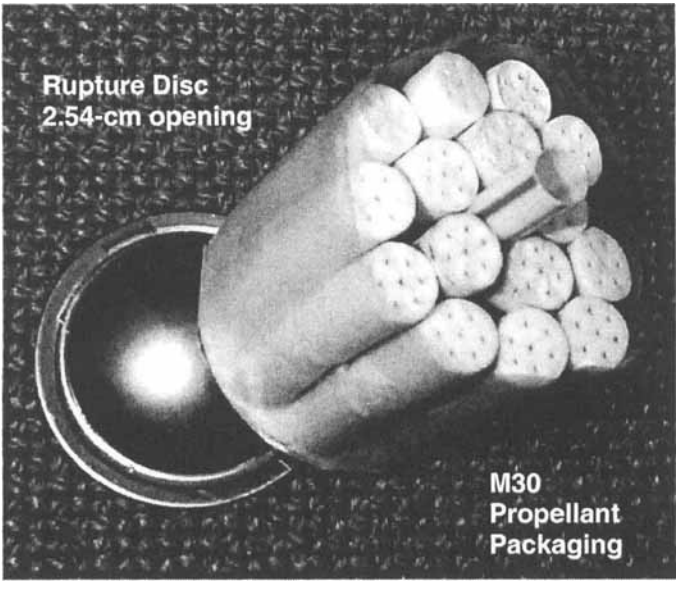

FIGURE 3.

Rupture Disk and an M30 Charge Used in Closed Bomb Experiments.

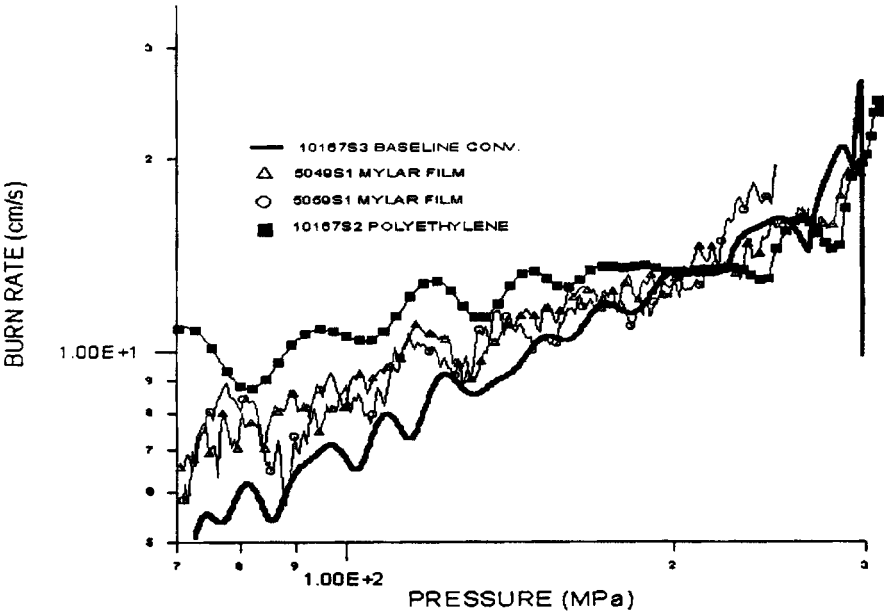

FIGURE 4.

Apparent Burning Rates of M30 Ignited with Mylar- or PE-Based Plasmas in Non-Interrupted Closed Bomb Trials.

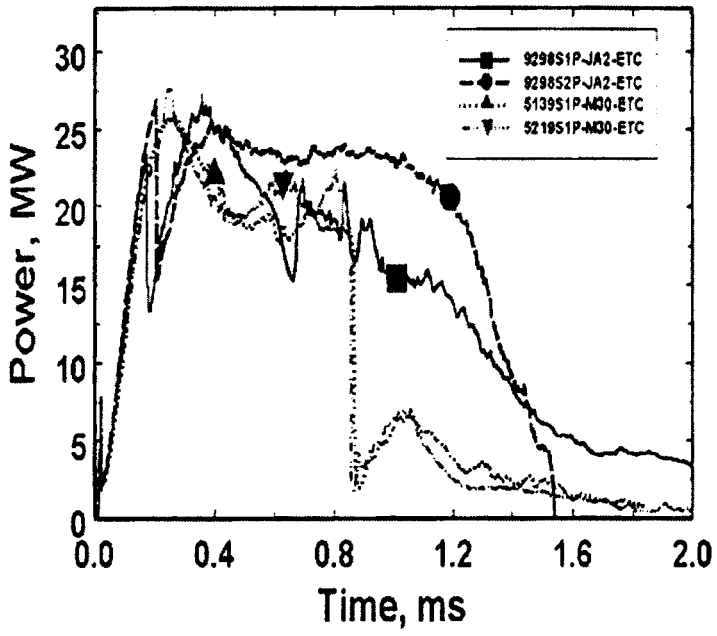

FIGURE 5.

Electrical Power Curve for Two Plasma Ignition Trials Yielding Different Input Energies (18.4 kJ and 29.3 kJ).

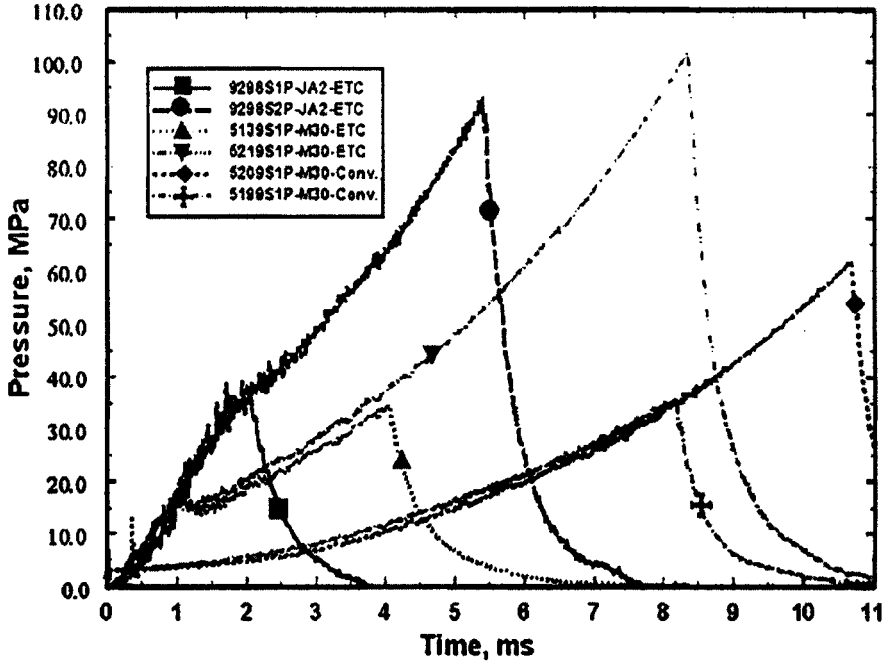

FIGURE 6.

Pressure-Time Curves for Plasma-Ignited M30 (Mylar Capillary) and JA2 (PE Capillary) Firings, and Conventional Firings for M30, for Interrupted Closed Bomb Trials.

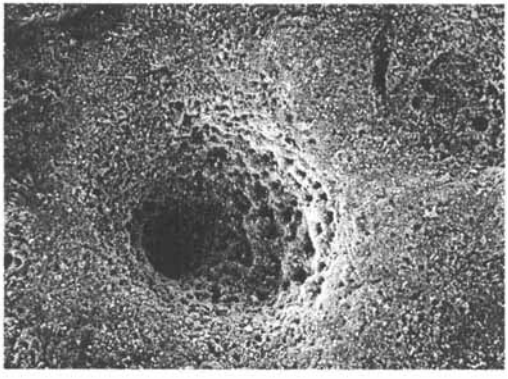

(90X)

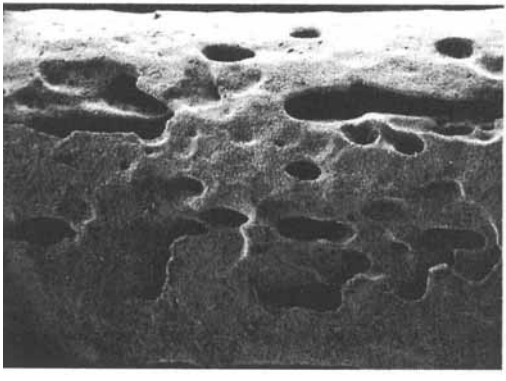

(5X)

FIGURE 7.

Micrograph of the Extinguished Grain Exterior Showing Evidence of Hot Particle Spray from the PE Plasma Igniter (100 MPa).

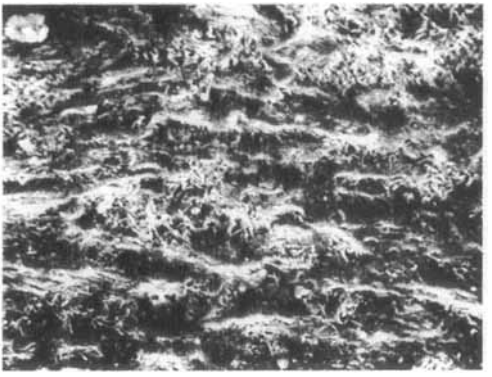

Conventional Ignition
(70 MPa, 850X)

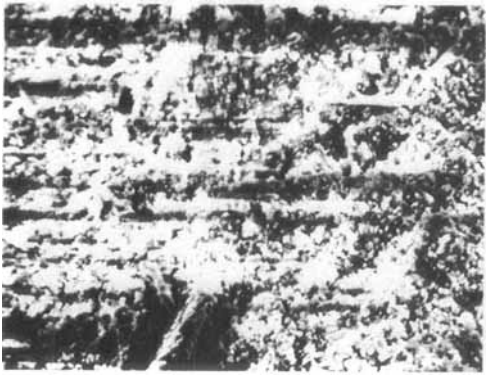

Plasma Ignition;
PE Capillary (35 MPa, 850X)

FIGURE 8.

Micrograph of the Burning Surface of the Extinguished Grain Perforation Showing Different Features Between Ignition Methods.

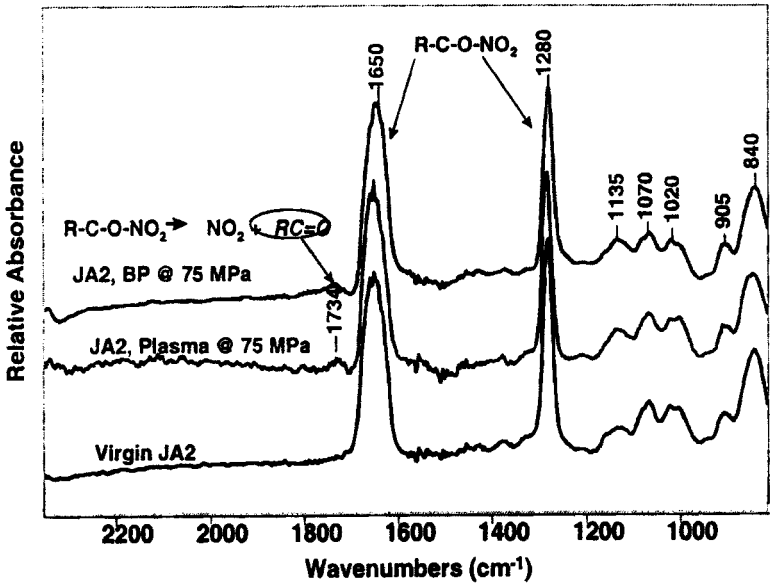

FIGURE 9.

FTIR Spectra of JA2 Showing Aldehyde Formation Due to Denitration of the Nitrate Ester Groups for Extinguished Samples.

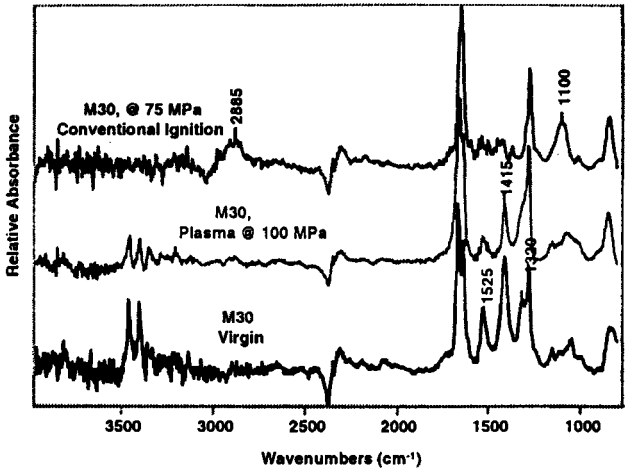

a

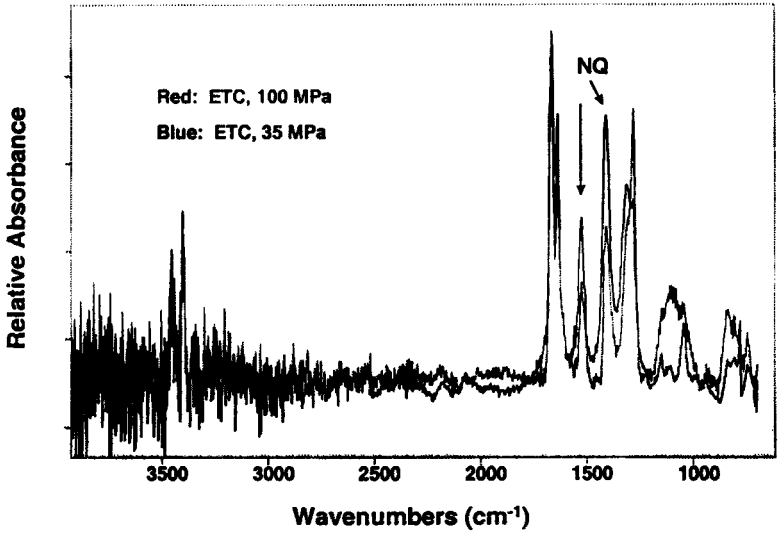

b

FIGURE 10.

Surfaces of Extinguished M30 Propellant Grains: a) Lateral Surfaces; b) Perforated Surface.

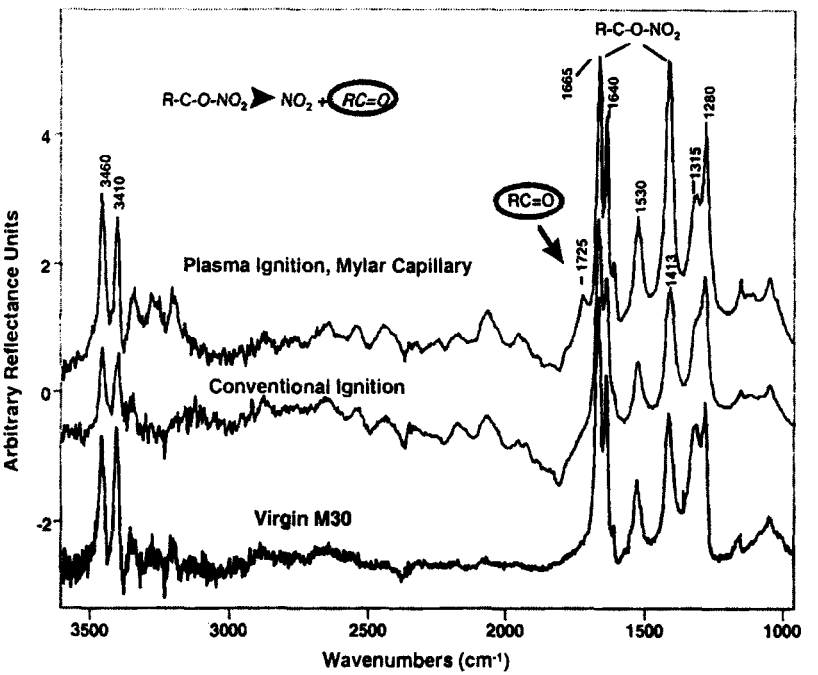

FIGURE 11.

Spectra of Outer Surfaces of M30 Grains Exposed to Both Conventional and Plasma (Mylar Capillary) Ignition; the Spectrum of a Cross-Sectioned Sample of Virgin M30 is Provided as Reference.

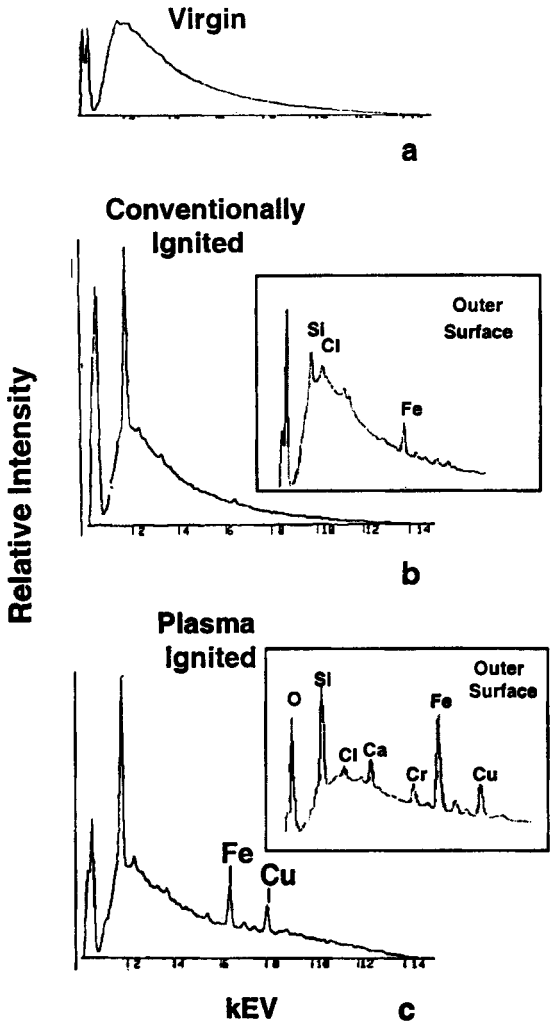

FIGURE 12.

XRF Analysis of M30 Grain Perforations: a) Virgin, b) Ignited with Black Powder, and c) Ignited with Plasma.